# Chapter 9
# Model Tests and Aero-hydrodynamic Simulation

## Introduction

Model testing is normally used to obtain performance characteristics for detailed design once a basic configuration has been selected, due to the complex geometry of a WIG craft and consequent three-dimensional airflow. Several model test series are carried out to analyse the different performance parameters, and provide the force coefficients or motion response operators that can then be used by scaling up to full size and inserting in the equations of motion for the WIG design. A static hovering platform, wind tunnel, ship towing tank and free running models in open water are all useful tools to gather data on the different aerodynamic and hydrodynamic characteristics.

Model test data for the whole craft can then be broken down into components by subtraction of elements that are predictable by analysis, such as lift and drag forces on the fin and tailplane, or from separate model tests of the main elements such as the wing. The remaining elements can then be related to the specific configuration and used directly in performance evaluation after scaling up to the prototype craft dimensions. Verification of the scaling relationship assumed initially, by comparison with full-scale trials of a prototype, is an important final step in the design process.

Scaling parameters for hydrodynamic model testing are similar to other high-speed marine vehicles and seaplanes, including Froude, Euler and Weber numbers. Aerodynamic data have to be obtained separately to hydrodynamic data due to the conflict between Reynolds and Froude numbers. It is not possible to model both at the same time, due to air being 800 times less dense than water.

In this chapter, we will summarise the scaling parameters, the tests that they can be applied to, and discuss results that have been obtained through WIG research at MARIC, including full-scale craft trials.

A separate issue to be addressed for WIG is how to deal with problems concerning the effect of structural elasticity on hydrodynamic and aerodynamic tests. Aerodynamic performance including the effect of structural elasticity is particularly important in WIG performance analysis due to the light-weight structure and significant hull and wing deformation – and the sensitivity of the aerodynamic characteristics to such flexure in the proximity to the ground. Structural stiffness can

L. Yun et al., *WIG Craft and Ekranoplan*, DOI 10.1007/978-1-4419-0042-5_9,

also affect hydrodynamic performance, though only to a minor extent, so that it can usually be ignored, and stiff models used. Modelling of cushion system characteristics, where flexible members are used, as in DACC, need to be addressed in the same way as other ACV modelling. The reader is referred to reference Chapter 2 [1] for guidelines on this aspect.

Procedures for testing WIG, as well as the relations between the various model experiments and theoretical analysis are also introduced in this chapter. Some problems that have occurred in MARIC model and theoretical investigations will be given as examples, and some remedial measures offered in this chapter for reference. We conclude with a short discussion of WIG concept design based on test data.

## Experimental Methodology

There are four experimental methods used for WIG hydrodynamic and aerodynamic studies (particularly for DACC and DACWIG) as follows.

### *Static Hovering Experiments on a Rigid Ground Plane*

Figure 4.11 shows static experiments on a rigid ground plane, and Fig. 4.21 shows the same tests for a full-scale craft over ground. In these tests, the static hovering characteristics such as clearance height and static stability can be investigated for DACC and DACWIG, and so evaluate the potential manoeuvrability over ground and during take-off. Such tests can also be used to study static characteristics of craft with separate lift fans if these are used for air cushion feed for DACC type craft, and their interaction with the propulsion and lift augmentation systems.

### *Model Tests in a Towing Tank*

These tests can obtain the resistance, running attitude (dynamic trim) and wave impact loads on a WIG model at low speeds at various positions of control surfaces (flaps, elevator, thruster guide vanes), CG and bow thruster speed, both on calm water and in waves.

Towing tank testing is the basic tool for estimating the craft performance before, during and after (but not far away from) take-off over calm water and in waves. In these tests, the aerodynamic forces are not measured. The model may be self-supporting on an air cushion (DACC or DACWIG), or suspended in the case of a WIG or PARWIG. In both cases, the model will be attached to the normal towing assembly installed on the towing carriage so as to measure the hydrodynamic forces and moments at various speeds and in different wave heights. The results will be a set of data to enable loads and moments within an envelope of sea states to be estimated for the full-scale craft, scaled using Froude's law.

## *Model Experiments in a Wind Tunnel*

In these tests, the aerodynamic properties, such as lift, drag, moment coefficients and derivatives of complete or half WIG models at various positions of flaps, rudders and elevators, guide vanes aft of bow propellers, trim angle, flying height, and drift angle of the model, can be investigated for the craft when flying in ground effect.

In addition, the dynamic properties of bow-thruster systems can be obtained for varying deflection of the jet into the main-wing cavity. Figure 4.10 shows a half model of a typical DACWIG in the wind-tunnel laboratory at MARIC.

Wind-tunnel tests are also used to determine the longitudinal and transverse stability parameters, and by subsequent analysis the manoeuvrability parameters (rate of turn for example), in a similar way to determination of aircraft manoeuvring performance [1].

Wind-tunnel models of the main lifting wing or the tail can also be tested to determine lift and drag coefficients for these components on their own, and with parametric variations to the geometry, test out such changes and identify the direction to optimise performance. The interaction of wings with the craft hull can also be investigated by comparison with data obtained from whole or half models of the craft.

In these tests, the air velocity used should be such as to keep the Reynolds number above $10^{-5}$ so as to ensure an appropriate degree of turbulent flow against the laminar flow over the model surfaces compared with the full-scale craft. Laminar flow would give very different data since the boundary layer is much thinner and the energy losses are so much lower. Small models may also give unrepresentative results if the breakaway for the turbulent boundary layer is too far back from the leading edge. Reference to aerodynamic texts such as Hoerner Fluid Dynamic DRag, and Lift, references Chapter 6 [10] and Chapter 7 [1], very helpful to give advice on these phenomena so as to assist modelling.

## *Radio-controlled Model Tests on Open Water and Catapult Model Testing Over Ground*

Figure 7.3 shows a radio-controlled model test on a lake. Although less experimental instruments and sensors can be mounted on these models due to their small size, such tests are very useful for qualitative analysis of WIG performance, particularly for testing the dynamic stability in flight. Since the model is small, the construction and operational cost of this test is low. Radio-controlled model tests are very useful in WIG research at the preliminary and concept design stage for this reason.

Care should be taken to interpret the results from such tests though, as Froude number will be high and Reynolds number may be low compared to the full-scale craft.

Catapult model tests have also been used for the qualitative study of longitudinal and transverse stability, as well as aerodynamic characteristics of WIG models. Such

tests are most suitable for investigating the aerodynamic configuration of novel WIG types during preliminary research. Models are made of GRP with a light hull and no engines, launched from the catapult, and flying in GEZ. Although the flight can only last for a few seconds, the running attitude can be observed briefly so as to judge the model stability. The test cost is very low, so a large number of aerodynamic configurations can be tested for parametric analysis [2].

Based on these tests, creative ideas for WIG design can be developed inexpensively, and the reliability and practicality tested with low risk, due to the un-powered and cost-effective nature of the models.

## WIG Model Scaling Rules

As with all marine vehicles, the model has to be an accurate geometric simulation of hull and wings, as well as key appendages on the craft, such as rudder, flaps and guide vanes. Based on the model geometric scale, the equivalent physical values for the full-size craft and model can be determined as in Table 9.1:

**Table 9.1** The equivalent size ratio of various physical value for the full size craft and model based on the geometric simulation

| Physical value | Symbol | Scale ratio |
|---|---|---|
| Length | $L$ (wing chord length, etc.) | $\lambda$ |
| Area | $S$ (air cushion area, wing area, etc.) | $\lambda^2$ |
| Weight and force | $F$(N) | $\lambda^3$ |
| Gravity acceleration | $g$ | Constant |
| Air and water density | $\rho$ | Constant |
| Air cushion pressure | $P_c$ (N/ m$^2$) | $\lambda$ |
| Speed | $V$ (craft speed, airflow speed, etc.) | $\lambda^{0.5}$ |
| Airflow | $Q$ | $\lambda^{2.5}$ |
| Power | $N$ (engine power, propeller power, etc.) | $\lambda^{3.5}$ |
| Frequency | $f$(vibration, wave encounter frequency) | $\lambda^{-0.5}$ |

where $\lambda$ is the linear scale ratio

## Scaling Parameters for WIG

### *Reynold's Number*

Reynold's number (Re) is the most important non-dimensional parameter for WIG performance prediction. In contrast to conventional high-speed marine craft, Re not only influences the drag forces on hull, wings, fin and tailplane, but also influences the lift forces on these same components. For this reason, Re affects the speed performance and also stability, manoeuvrability and operational safety. The influence of Re on performance of different components of a WIG is as follows.

**Reynold's Number of Bow-Thruster Jet Flow**

$$\mathrm{Re}_1 = V_\mathrm{j} t/\nu,$$

where

| | |
|---|---|
| $V_\mathrm{j}$ | Jet velocity |
| $t$ | Average thickness of the jet nozzle |
| $\nu$ | Kinetic coefficient of viscosity |

This Reynold's number relates to scaling of the mixture of jet flow and its surrounding air from the jet nozzle to the entrance of the air channel. The greater the Re, the larger is the external volume flow mixed into the jet and the higher the air cushion pressure generated.

According to Krause and Gallington, Chapter 1 [10], the effective static cushion pressure generated can be expressed as:

$$P_c/q_\mathrm{j} = f\left(\overline{h}, \mathrm{Re}_1\right) \tag{9.1}$$

where

| | |
|---|---|
| $P_\mathrm{c}$ | Effective static air cushion pressure under main wing |

$q_\mathrm{j} = 1/2\rho_\mathrm{a} V_\mathrm{j}^2$ pressure due to jet flow

**Reynold's Number of Bow-Ducted Air Propeller Blades ($\mathrm{Re}_2$) and Duct ($\mathrm{Re}_3$)**

$$\mathrm{Re}_2 = V_\mathrm{p} B/\nu_\mathrm{a}$$

$$\mathrm{Re}_3 = V_\mathrm{o} L/\nu_\mathrm{a} \tag{9.2}$$

where

| | |
|---|---|
| $V_\mathrm{p}$ | Resultant velocity of flow on the propeller blade |
| $B$ | Blade width |
| $V_\mathrm{o}$ | Axial velocity of flow in propeller disc |
| $L$ | Length of duct |
| $\nu_\mathrm{a}$ | Relative viscosity of air |

The Reynold's number at the blade/duct of model and full-scale craft are different, and sometimes there may be a larger difference between different scale models than model to full scale. Table 9.2 shows $\mathrm{Re}_2$ of two models and a full-scale craft.

**Table 9.2** $Re_2$ of the models and a full-scale craft

| | Model No. 1 | Model No. 2 | Full-scale craft |
|---|---|---|---|
| $Re_2$ | 5.2E5 | 1E6 | 2.5E6 |
| Scale ratio ($\lambda$) | 1/13 | 1/6.5 | 1 |

The models simulate the full-scale craft geometry, for hull, wings and appendages. In addition, the thrust of the models is also simulated. However, sometimes it is found that the maximum lift–thrust ratio (i.e. the ratio of maximum lift and rated thrust of bow thrusters when the model has just taken off from ground) for the models and full-scale craft are rather different. Errors can therefore occur during the design of the WIG if the lift–thrust ratio is used as an aerodynamic scaling criterion, as Dr. Kraus and Dr. Gallington suggested.

Sometimes, it is found that the lift–thrust ratio for models, particularly for small-size models, is too high to achieve on full-scale craft. This is due to the different Re of the models and full-scale craft.

Figure 9.1 shows the maximum lift of a rectangular airfoil as a function of Re, where the thickness to chord ratio is 12%. The figure shows the general tendency of lift coefficient with respect to Re.

Figure 9.2 shows the lift comparison at low Re, it is found the influence of Re on the lift coefficient is very large, particularly at lower Re.

Figure 9.3 shows the lift–drag characteristic of thin section airfoils at low turbulence and Re; it can be seen that the aerodynamic performance of the airfoils with larger Re is much better than that with lower Re.

Figure 9.4 shows the lift coefficient of an N-60 two-dimensional airfoil versus various Re and changing trim angles [1]. The author was trying to understand why

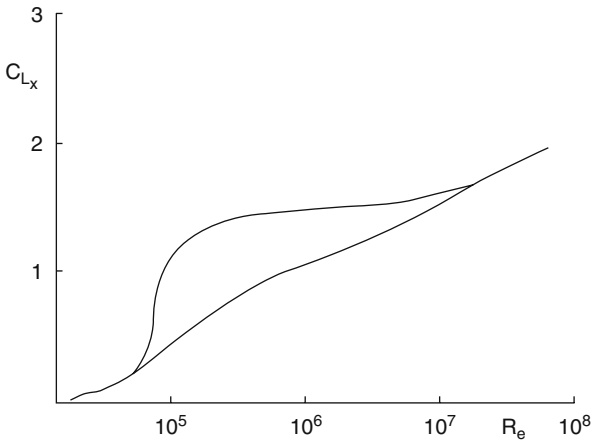


**Fig. 9.1** Maximum lift of a rectangular airfoil as a function of Re

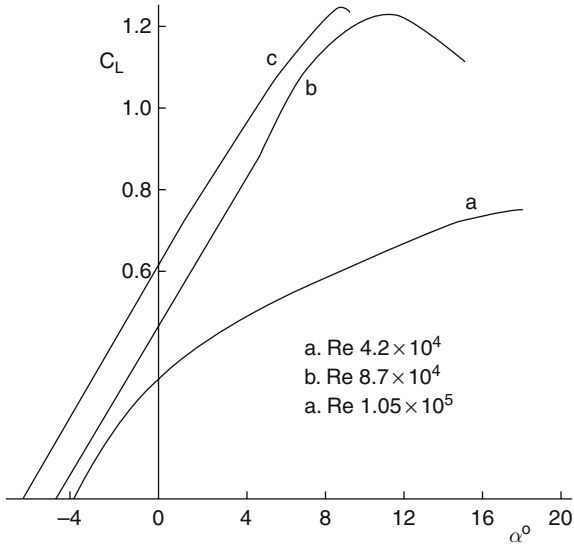


**Fig. 9.2** Lift comparison at low Re

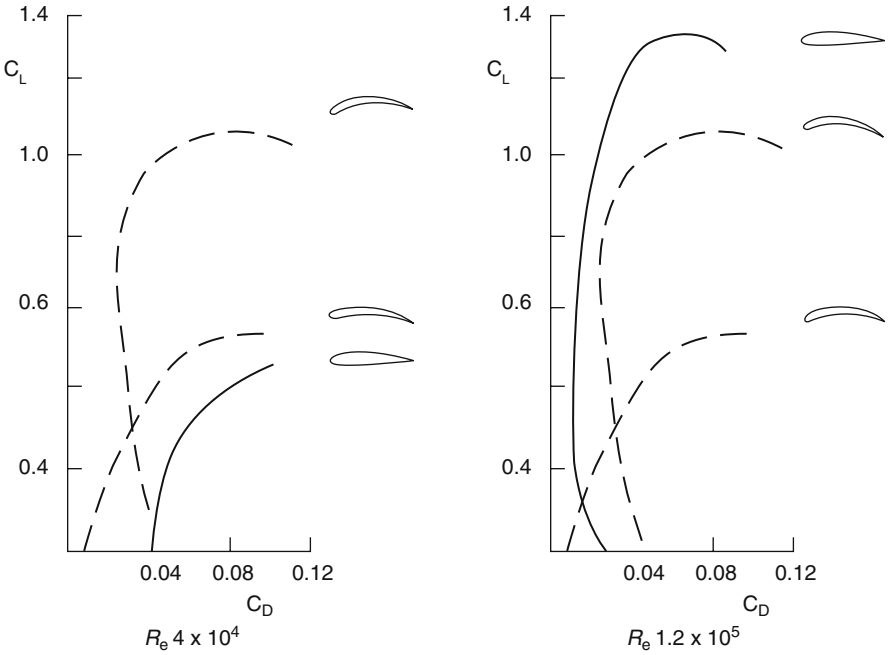


**Fig. 9.3** Lift–drag characteristics of thin section airfoil at low turbulence and Re

the lift coefficient, aerodynamic properties and longitudinal stability of a model airplane are poor compared to the full-scale aircraft, particularly at small scale. From the figure, it can be seen that the lift coefficients drop rapidly with a decrease in Re, particularly in case of Re lower than $1 \times 10^5$ (1E5). The curves from 1 to 6 in Fig. 9.4 below show Re$1.47 \times 10^5, 1.05 \times 10^5, 8.4 \times 10^4 6.3 \times 10^4, 4.2 \times 10^4$ and $2.1 \times 10^4$, respectively.

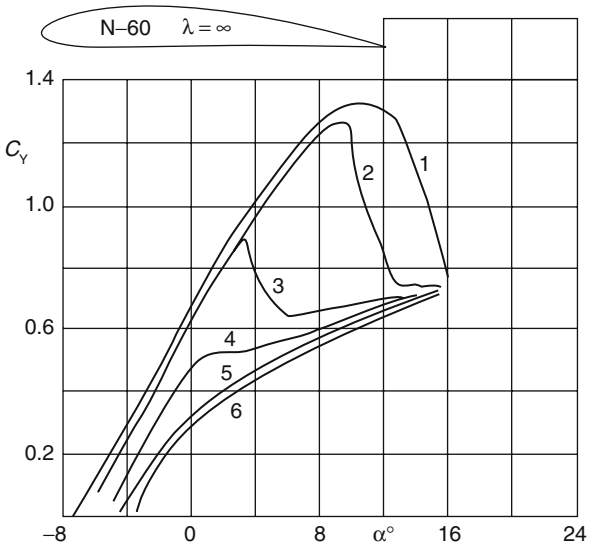


**Fig. 9.4** $C_{Lmax}$ versus Re for N-60 aerofoil

Figures 9.5 and 9.6 show both drag and lift coefficients of four airfoil profiles (NACA 6412, 2412, 4412 and 0012) with respect to Re. It is found that both drag and lift coefficients decrease with Re; however, the lift coefficient drops more rapidly than the drag coefficient. This may be why the aerodynamic properties of airplane and WIG models are worse than those of full-scale craft.

If the model Re is closer to the real craft value, the lift–thrust ratio and model aerodynamic properties more closely resemble the full-scale craft. For this reason, it is suggested that WIG models have to be large enough to obtain Re larger than $1 \times$ E6, otherwise great care is needed when using the lift–thrust ratio as a scaling criterion for estimating the lift power of real craft due to the distortion of model lift coefficient.

A designer can also use the parameter $P_c/q_j$ (where $P_c$ is the cushion pressure and $q_j = 1/2\rho_a V_j^2$) as a scaling criterion for predicting the lift power and functional requirements of bow thrusters, such as the overall pressure head and lift propeller flow rate in static hovering mode, particularly in case of small model with lower Re ($Re_1$ lower than critical Re). The cushion pressure is established from the total pressure head delivered by the lift air propeller, rather than the propeller thrust. The lift provided by the cushion under the wing is reduced compared to a fully contained air cushion by the decaying pressure pattern under the outer wing away from the

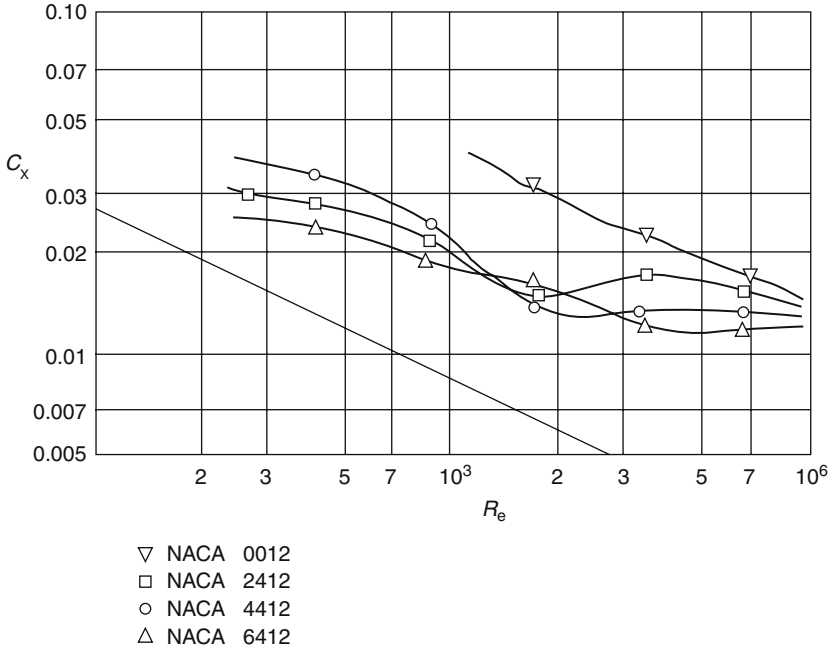


**Fig. 9.5** $C_y$ versus Re for different aerofoils NACA 00/24/44/64 – 12

thruster feed, where air leaks away into the free air stream. Increasing the forward speed reduces this decay, increasing the air gap under the cushion, until take-off occurs and ground effect can be utilised fully for support.

### Reynold's Number of the Tailplane, Fin and Rudder ($Re_4$)

Reynold's number is particularly important for the tailplane and elevators, which strongly influence the longitudinal stability.

$$\mathrm{Re}_4 = V_s L_r / \nu_a \tag{9.3}$$

where

$V_s$ Craft speed
$L_r$ Chord length of tailplane or fin/rudder

The tailplane is the key component for maintaining positive longitudinal stability and vertical force balance about the WIG CG in flying mode. Determination of the correct angle of attack for installation of the tailplane is therefore essential. Figure 9.7 shows the relative aerodynamic centre $X_{dc}$ versus tailplane installation angle of attack $\Pi$ of a typical DACWIG model. It can be seen that the larger the

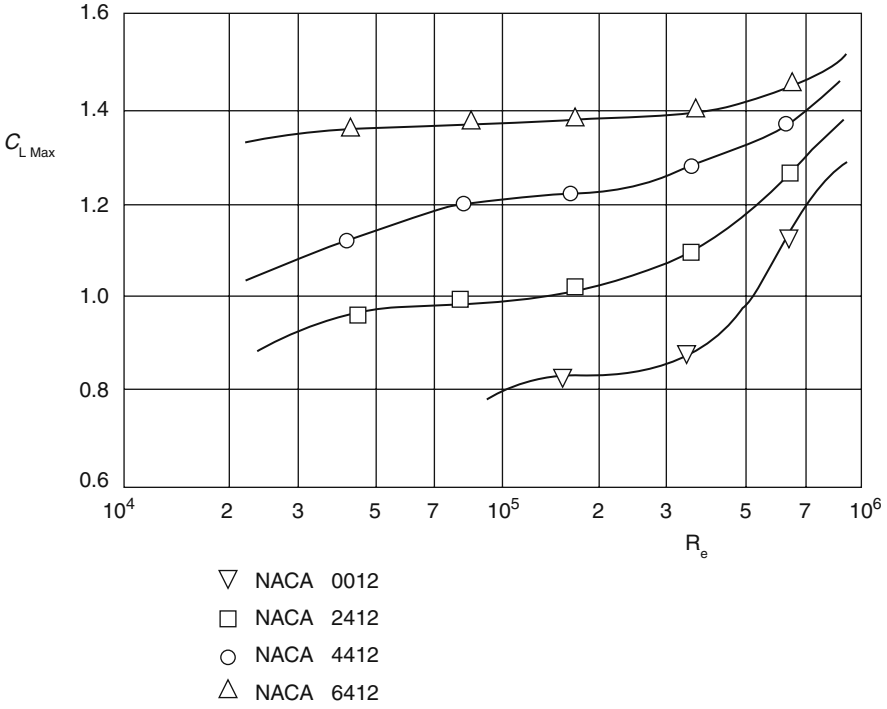


**Fig. 9.6** $C_x$ versus Re for different aerofoils NACA 00/24/44/64 – 12

horizontal angle downward, the more the equilibrium CG of the craft model moves rearward, as the lift force on the tailplane increases.

Figure 9.8 shows the relative pitching moment versus the aerodynamic lift coefficient $C_y$ of a DACWIG from a wind-tunnel model test with two different tailplane

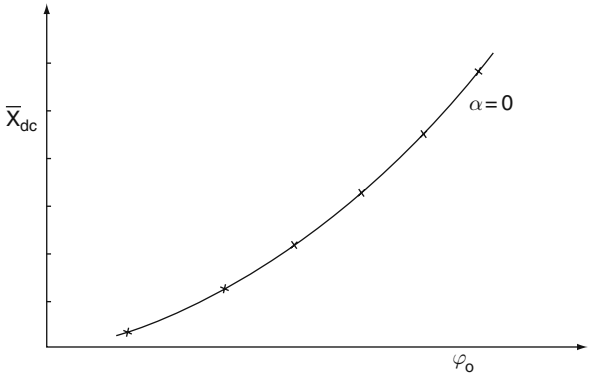


**Fig. 9.7** Relative aerodynamic centre $X_{dc}$ versus installed angle of horizontal stabilizer of a typical DACWIG model

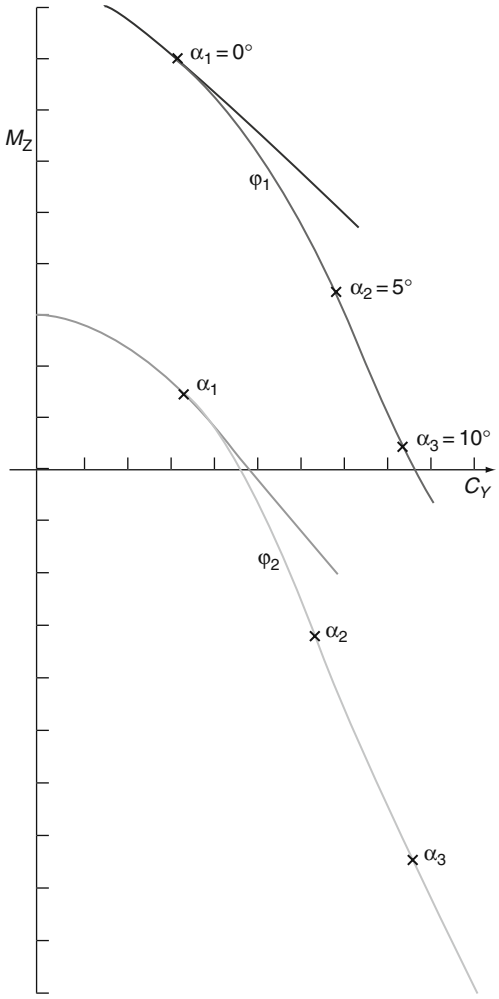


**Fig. 9.8** $M_Z$ versus $C_y$ of a typical DACWIG model

installation angles, $\prod_1$ and $\prod_2$. During this model test, the relative flying height $\overline{h}$ is in strong GEZ, flap opened fully, and guide vanes turned horizontal, which is a typical position of controls for a DACWIG flying after take-off.

The slope of these curves represents the longitudinal position of the aerodynamic pitching centre (or aerodynamic centre of lift increment) with respect to the trim angle, $\overline{X}_{F9}$. From Figs. 9.7 and 9.8, it can be seen that the tailplane angle of attack strongly affects $\overline{X}_{F9}$ and also the aerodynamic centre of lift increment due to pitch for the model.

One question is whether the model test results will be representative at full scale. Table 9.3 shows an example of $Re_4$ for models and a full-scale craft.

**Table 9.3** $Re_4$ for different models and full-scale craft

| | Model No. 1 | Model No. 2 | Full-scale craft |
|---|---|---|---|
| Scale ratio | 13 | 6.5 | 1 |
| $Re_4$ | 5E4 | 1.4E5 | 1.95E6 |

The value of model No. 1 $Re_4$ is too small to correctly model tailplane stabilizer and rudder lift coefficient. It is found that the difference between experimental and two-dimensional data (infinite AR) from tests at high Re of standard airfoil forms is significant. Sometimes the 2D value is as large as twice that of test results for WIG. This is mainly due to the difference in Re. Remedial measures for improving the design data for stability and longitudinal force balance are

- Use a larger model with $Re_4$ larger than critical Re (approx. 1E5)
- Adjust the installed angle of full-scale craft tailplane to compensate the difference of lift coefficient between model and full-scale craft

## *Euler Number ($H_q$) and Relation to Cushion Pressure Ratio*

In order to simulate the external aerodynamics of a WIG craft in a wind tunnel, the cushion pressure ratio has to comply with

$$\mathrm{H_q} = P_c / \left(1/2\rho_\mathrm{a} V_\mathrm{a}^2\right) \tag{9.4}$$

where

$P_\mathbf{c}$ Cushion pressure in the air channel ($N/m^2$)
$V_\mathbf{a}$ Air velocity (m/s)

According to Table 9.1, $V_\mathrm{a} \propto \lambda^{0.5}$, so the air speed in the tunnel is similar to the craft speed in the towing tank and $\mathbf{H_q}$ is similar to Fn.

## *Wind-Tunnel Testing*

During model testing of WIG in a wind tunnel, after ensuring that Re is modelled correctly, the tunnel surface under the WIG model should ideally be a moving belt of some kind running at the same speed as the airflow or craft speed. This then avoids unwanted boundary layer effects from a static tunnel surface that will cause unrealistic flow in the area under the main lifting wing and make it difficult to analyse the internal and external aerodynamic characteristics.

A rolling ground is not a standard feature in wind tunnels, so alternative methods may have to be used if one cannot be fitted. Three possible approaches are considered first. Figure 9.9 shows the airflow velocity distribution under the wings for WIG tests in a wind tunnel with three types of supported rigid ground [2]. If the wing speed is $V_c$ (i.e. airflow speed in the wind tunnel), then the velocity distribution of the right side of Fig. 9.9 is with respect to the fixed earth coordinate system and the left part with respect to the coordinate system fixed on the wing. Figure 9.9a shows the velocity distribution for the real moving wing of WIG model or craft, and Fig. 9.9b the velocity distribution for a wing in a wind tunnel with fixed boundary surfaces. Since the ground surface is static, the boundary layer influences the velocity distribution of both wing and ground. Figure 9.9c shows the velocity distribution of wing and ground when using the method of wing image, i.e. putting an identical model opposite to the original wing model to eliminate the rigid ground and the boundary layer influence.

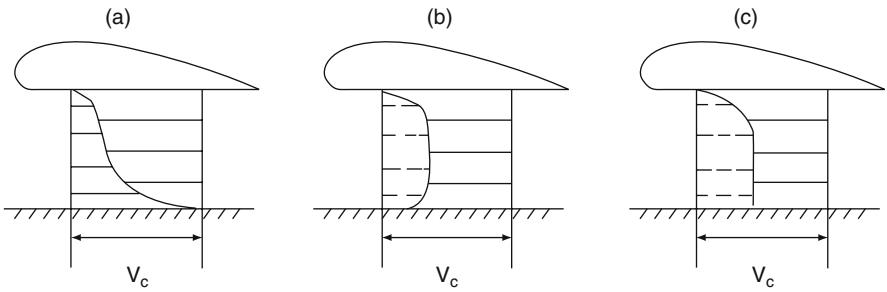


**Fig. 9.9** The velocity distribution of airflow under the wings for WIG test in wind tunnel with three types of supported rigid screen

Figure 9.9a shows the real moving wing velocity distribution, i.e. the velocity at the ground is equal to zero and $V_c$ on the wing. The difference between wing and ground is equal to $V_c$. However, in Fig. 9.9b, the speed difference is zero, and in Fig. 9.9c between 0 and $V_c$.

Methods (b) and (c) do not correctly simulate the ground boundary velocity. As a result, significant errors in prediction of the wing lift coefficient $C_y$ will occur; too small for (b) and too large for (c). For this reason the Krylov Ship Research Institute (KSRI) in Russia has established a large wind tunnel with a moving ground as shown in Fig. 9.10, to eliminate the test errors mentioned above and obtain more precise test results for WIG [3]. Figure 9.10a shows the overall arrangement, including the moving ground plate arrangement with circulating belt and static leading edge. The ground plate is supported on hydraulic jacks for adjusting the ground level and angle, see Fig. 9.10b.

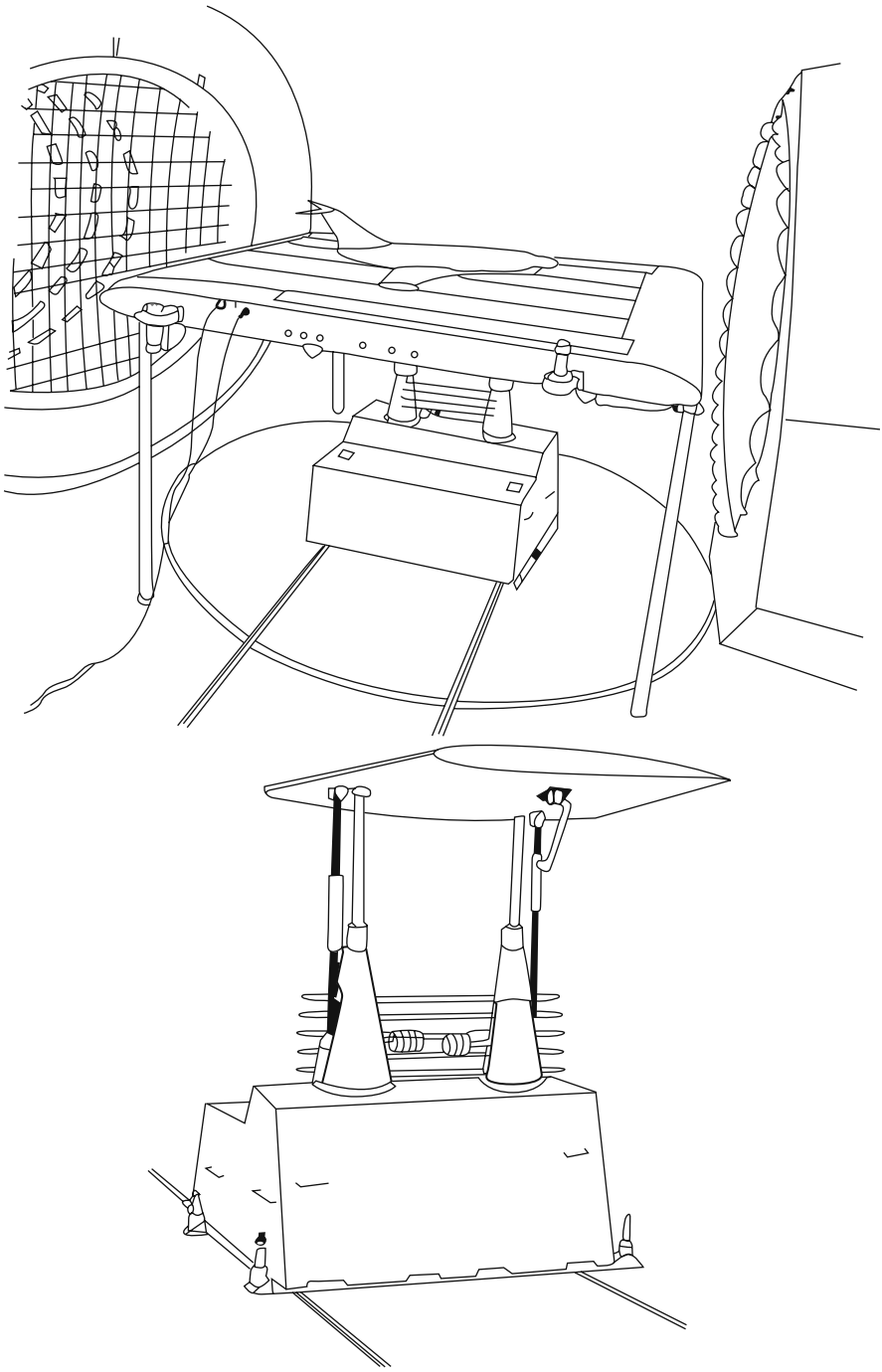

**Fig. 9.10** "Moving screen" equipment in wind-tunnel laboratory of KSRI of Russia

The leading particulars of the KSRI wind-tunnel laboratory are as follows:

| | | |
|---|---|---|
| Dimensions of working section of the wind tunnel | $4 \times 4 \times 2.3$ | m |
| Maximum wind speed | 100 | m/s |
| Velocity field non-uniformity | <1% | |
| Maximum down wash and lateral wash angle | $\pm 0.3, \pm 0.5$ | degrees |
| Maximum Re (for full craft model) | 2 E7 | |
| Linear velocity of moving ground | 30 | m/s |

An alternative method, a fourth approach, aimed at decreasing the boundary layer influence on a static ground plate is to make two slots in the ground plate connected to small suction fans and also mount two disturbance plates under the slots so as to make a turbulent flow and a suction field under the slots. The boundary layer thickness can then be reduced effectively. Figure 9.11 shows a general arrangement of the slots and disturbance strakes in a wind tunnel, the dimensions of which are: test section length 1.95 m and test section diameter 1.5 m. Two slots are located at 800 mm and 1,200 mm from the leading edge of the ground plate, respectively, with a width of 30 mm. The inclination angle of the disturbance strakes is 60°.

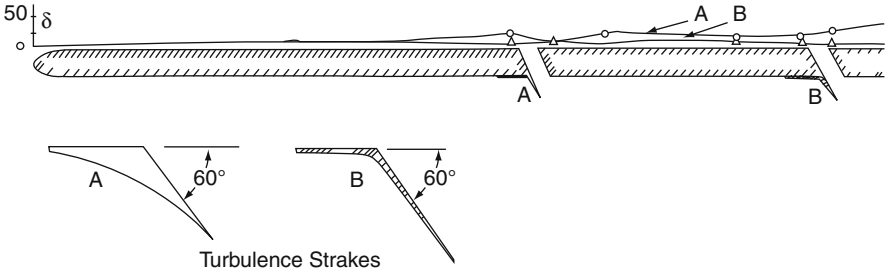


**Fig. 9.11** The distribution of boundary layer thickness on the rigid screen of the wind-tunnel facility

The turbulence generator strakes have to be made with knuckles to give more effective turbulent flow under the slots as shown in Fig. 9.11. Boundary layer thickness at the rear part of the plate can be reduced to as low as 10 mm for the knuckle-type turbulence strake, but 55 mm for the smooth-type turbulence strake. The calculated boundary layer thickness without the turbulence equipment is about 30 mm so the equipment is useful for reducing the boundary layer influence in the wind-tunnel laboratory.

## *Bow Thruster or Lift Fan Non-dimensional Characteristics of DACC and DACWIG*

The bow thruster non-dimensional characteristic is most important for correctly simulating static hovering performance, speed performance, longitudinal stability,

take-off, wave impact loads on the hull, etc. Since the bow thruster can be either a ducted air propeller or an axial fan, two types of scaling criteria can be used as follows.

**Air Propeller Type**

$$K_t = f\left(\lambda_{\mathrm{p}}, \mathrm{Re}\right) \tag{9.5}$$

where

$$K_{\mathrm{t}} = T/\rho_{\mathrm{a}} n^2 \mathrm{D}^4$$

$$\lambda_{\mathrm{p}} = V_s/Dn,$$

the influence of Re has been discussed in the previous section.

- $T$ Thrust of the air propeller (N)
- $\rho_{\mathrm{a}}$ Air density (N s/m)
- $n$ Propeller speed (r/s)
- $D$ Diameter of propeller (m)
- $K_{\mathrm{t}}$ Thrust coefficient of propeller
- $\lambda_{\mathrm{p}}$ Advance ratio of propeller

In this case, if the non-dimensional thrust characteristic is correctly modelled, the lift–thrust ratio can be used as a design criterion for predicting the static hovering performance of the WIG.

**Ducted Fan Type**

$$\overline{H}_{\mathrm{j}} = H_{\mathrm{j}}/\left[\rho_{\mathrm{a}} n^2 D^2\right] \tag{9.6}$$

$$\overline{Q} = Q/\left[nD^3\right] \tag{9.7}$$

where

- $\overline{H}_{\mathrm{j}}$ Non-dimensional pressure coefficient of ducted fan
- $\overline{Q}$ Non-dimensional flow coefficient of ducted fan
- $H_{\mathrm{j}}$ Overall pressure of fan (N/m)
- $Q$ Flow rate of fan (m/s)
- $N$ Fan speed (r/s)
- $D$ Diameter of fan impeller (m)

The fan-specific speed can be written as follows for selecting the type of fan in preliminary design.

$$\mathrm{Ns} = \left(\overline{Q}\right) / \left(\overline{H_{\mathrm{j}}}\right)^{0.75} \tag{9.8}$$

In model experiments, it is difficult to satisfy this criterion due to the higher speed of model electric motors. In this case, one can take lift–thrust ratio as the design scaling criterion in the case of Re larger than critical Re, otherwise take Euler number $H_q$ as the design scaling criterion.

## *Froude Number, Fn*

From Chapter 7, WIG total drag before and around the take-off speed is expressed as:

$$R = R_{\mathrm{hw}} + R_{\mathrm{sww}} + R_{\mathrm{aw}} + R_{\mathrm{hf}} + R_{\mathrm{swf}} + R_{\mathrm{a}} + R_{\mathrm{fl}} \tag{9.9}$$

The main drag force in this mode is wave-making drag caused by hull, sidewall and air cushion. In addition, the friction drag of hull and side buoys depends on the craft's running trim. In short, WIG drag before take-off is similar to that of an SES or hydroplane. This drag force characteristic can be obtained by model experiments in a towing tank. Scaling of the forces will then be carried out using the Froude number Fn as the criterion.

$$\text{Where } \mathrm{Fn_c} = V_s/\sqrt{gC} \text{ or } \mathrm{Fn_d} = V_s/\sqrt{gw^{\frac{1}{3}}} \tag{9.10}$$

$V_s$ Craft speed (m/s)
$C$ Wing chord (m)
$W$ Craft displacement ($m^3$)

## *Weber Number, We*

During the investigation of WIG spray formation, the relation between inertia force and surface tension of water has to be taken into consideration. The size and direction of the spray droplets are a function of We, where

$$\mathrm{We} = \left(\rho_w V^2 L\right) / \sigma_s \tag{9.11}$$

where

$\rho_w$ Density of water ($N\ s^2/m^4$)

$V$ Speed of water flow (m/s)
$\sigma_s$ Surface tension of water (N/m)

Since $\sigma_s$ and $\rho_w$ for both model and full-scale craft are constant, then $We \propto \lambda^2$, $We_s \gg We_m$. This means that spray from full-size craft will be significantly greater than at model scale, and the spray droplets on the full-scale craft will be much finer than that of a model.

This phenomenon has been observed during testing of model and full-scale craft, which affect the spray drag and pilot vision as well as the water spray ingestion into the bow engines.

On the Orlyonok WIG, there are turbojet engines mounted in the fuselage nose as bow thrusters. The higher the speed of the exhaust gases from the engine's nozzle, the more intense is this cloud of spray. Jet engines produce the largest spray cloud while the air propeller engine produces smaller such clouds. The process of water spray generation due to "under wing gas-air jets" on some WIG craft, like the Orlyonok, cannot be simulated in model experiments, so the analysis of full-scale trails data is important for such designs. So far there is no published data available.

## *Other Scaling Terms for Towing Tank Test Models*

From Chapter 7 , we have the total resistance of WIG; $R$ is equal to the measured drag plus the effective thrust of bow propellers as follows:

$$R = R_t + T_d.\eta_{Td} \tag{9.12}$$

$$\eta_{Td} = (R_{a3} - R_{a2}) / T_d \tag{9.13}$$

$$\eta_{Td} = f\left[V_{jo}/V_s, V_r/V_{jo}, \gamma, \beta, \vartheta, \overline{h}\right] \tag{9.14}$$

The critical data to obtain from wind-tunnel tests is the thrust recovery coefficient. In Equation (9.13), $R_{a2}$ and $R_{a3}$ represent the air drag of the model without bow thruster and with rotating bow thrusters, respectively. However, both $R_{a2}$ and $R_{a3}$ are large values with similar accuracy (or inaccuracy ...). According to the theory of probability, the result of subtraction of two large test values is a value with a large error. For this reason, it is difficult to obtain a precise thrust-recovery coefficient from wind-tunnel testing.

Equation (9.14) proposes that $\eta_{Td}$ is a function of various parameters, such as

$V_{jo}$ Speed of jet flow after the bow propeller
$V_s$ Craft speed
$V_r$ Airflow speed at the trailing edge exit under the main wing
$\gamma, \beta$ Angle of flap and thruster guide vanes, respectively
$\vartheta$ Craft trim angle
$\overline{h}$ Relative flying height

It is also very difficult to determine the thrust-recovery coefficient by calculation. Perhaps the best way to obtain $\eta_{\mathrm{Td}}$ is to put a strain gauge probe on the bow thruster to test the thrust directly.

$$\text{Then } R = R_t + \mathrm{T_d} \tag{9.15}$$

where

$R$ Total resistance of the model
$R_\mathrm{t}$ Measured resistance of the model
$T_\mathrm{d}$ Dynamic thrust of the bow propellers

### *Structural Simulation*

It is not possible to scale the structural rigidity of the model from the real craft. In general, the structural rigidity of a model is much greater. The structural deformation at full scale will be significantly greater than that of the model due to the scale effect. In addition, since the static hovering height (i.e. the gap between the ground and base plane of both main hull and side buoys during craft static hovering) is rather small, the structural deformation will significantly influence the craft aerodynamic properties, particularly in case of static hovering. The aero-elasticity effect will thus influence the model aerodynamics particularly in tests of amphibious characteristics.

Figure 9.12 shows the hull and sidewall structural deformation of a typical DACC or DACWIG, exaggerated. It is assumed that the aerodynamic lift is acting on the main wing uniformly, and most of the craft weight is concentrated in the main hull. During static hovering, the main wing is deformed upward and main hull downward, consequently significant cushion flow leaks outward under the side buoys and outer wing section trailing edge, while the hull still touches the ground. Higher cushion airflow is required to give a particular hovering height for the full-scale craft than predicted by model tests, as the model will be stiffer than the full-scale WIG. This needs to be corrected by analysis of the full-scale craft wing deflection when hovering, and additional airflow provided to account for this.

The deformation of the structure will be higher on a riveted hull structure compared to a welded aluminium hull due to the small movements of rivets in their joint holes on the plates of the craft and so this influences the aero-elastic properties of the craft. Since riveted structure would normally be selected so as to design for strength rather than stiffness, it would be natural for greater flexibility to be present. This may influence the designers' choice of structural design for the hull and main-wing section for a WIG, so as to obtain the stiffest possible structural configuration.

## Scaling Criteria

Some of the scaling criteria and terms discussed above, which have to be complied with in the model experiments, are listed in Table 9.5, where $\lambda$ represents the linear scale ratio.

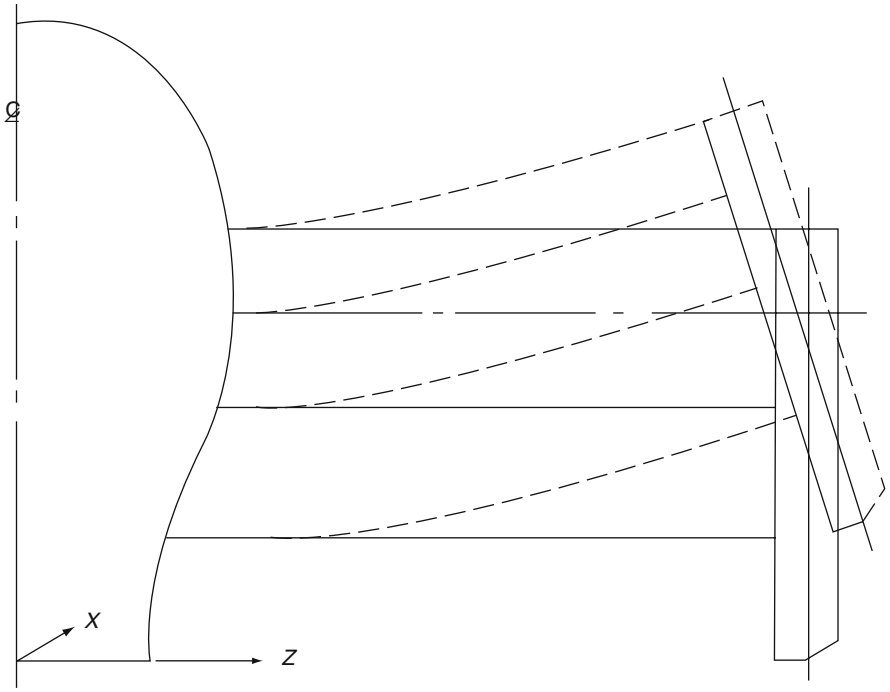


**Fig. 9.12** Deformation of the structures of typical DACC and DACWIG in static hovering

## Model Test Procedures

A flow chart showing typical model experimental investigations of the aerodynamics and hydrodynamics of WIG and how they fit into the design sequence is shown in Fig. 9.13

There are three main tests to be carried out as follows:

- Static hovering test of the models over ground (including a few tests of model clearing obstacles on ground)
- Wind-tunnel aerodynamic tests on rigid ground plate, either moving or with boundary layer control slots
- Hydrodynamic test in a towing tank and radio remote control self-propelled model tests in open water, as well as manned craft tests

The relation between the three test series and between these experimental investigations compared to theoretical calculation is illustrated in Fig. 9.13.

**Table 9.5** Scaling criteria and terms to be complied with in WIG model experimental testing

| Item | Simulation criteria | Used in what kind of tests | Practical possibility | Degree of influence | Remarks |
|---|---|---|---|---|---|
| 1 | $Re_1$ (Re with respect to jet flow after bow thrusters) | (1) Static hovering on ground<br>(2) Wind-tunnel test<br>(3) Radio remote control model free flying<br>(4) Towing tank tests | 1. Impossible<br>2. $Re_1 > Re_c$ | On the mixture of airflow Medium | |
| 2 | $Re_2$, $Re_3$ (Re with respect to bow ducted air propeller blades and duct) | (1),(2),(3),(4) | 1. Impossible due to high speed of electric motor<br>2. $Re > Re_c$ | 1. Very high influence on (1)<br>2. High influence on others | 1. Enlarged model for $Re > Re_c$ |
| 3 | $Re_4$ (Re with respect to stabilizers and rudders) | (2),(3),(4) | 1. Very difficult<br>2. $Re > Re_c$ | 1. Strong affect to stability of running model<br>2. Lead to misunderstanding the stability of design craft | 1. Enlarged model for $Re > Re_c$,<br>2. Otherwise, carefully designing the stabilizers and rudders of real craft |
| 4 | Non-dimensional characteristics of bow air propeller $K_t$ | (1),(2),(3),(4) | 1. Possible, if $Re_2 > Re_{c2}$<br>2. Otherwise, no use | Great influence on all tests, particularly (1) | Enlarged model for $Re > Re_c$ |
| 5 | Non-dimensional characteristics of bow lift fan $\overline{H}_j$,$\overline{Q}7$ | (1),(2),(3),(4) | 1. Possible if $Re_2 > Re_{c2}$<br>2. Otherwise, no use | Great influence on all tests, particularly (1) | Enlarged model for $Re > Re_c$ |
| 6 | Euler number $H_q$ | (1),(2),(3),(4) | Possible | Great | |
| 7 | Lift–thrust ratio $= W/T_o$ | (1),(2),(3),(4) | 1. Possible if $Re_2 > Re_c$<br>2. Otherwise, take $H_q$ as the design criterion | Great influence, particularly on static hovering performance | Enlarged model for $Re_2 > Re_c$ |

**Table 9.5** (continued)

| Item | Simulation criteria | Used in what kind of tests | Practical possibility | Degree of influence | Remarks |
|---|---|---|---|---|---|
| 8 | $V_g = V_s$, where $V_g$ is the linear moving speed of rigid ground in wind tunnel | (2) | Possible, but too expensive | Medium | If no moving ground, take slot equipment on ground |
| 9 | Fn | (3),(4) | Possible | Great | |
| **Item** | **Simulation criteria and terms in tests** | **Used in what kind of tests** | **Practical possibility** | **Influence degree** | **Remarks** |
| 10 | We | (3),(4) | Impossible | Influences spray forming | |
| 11 | Thrust-recovery coefficient, $(R_{a3} - R_{a2}) / T_d$,where $T_d$ is the dynamic thrust on a single thruster separated from the craft, $R_{a3}$ is the drag of model with rotating bow thrusters and $R_{a2}$ drag of bare model | (2),(4) | 1. In wind-tunnel test, it can be taken, but not precise<br>2. In towing tank, strain gauge probes can be taken for measuring the dynamic thrust of bow thruster on model | Medium | (1) Is possible, but not precise<br>(2) Rather difficult to mount |
| 12 | Aero-elastic simulation Structure problems | (1),(2),(3),(4) | Impossible | Great influence on (1) | If according to model test data, carefully predicting the static hovering height of real craft |

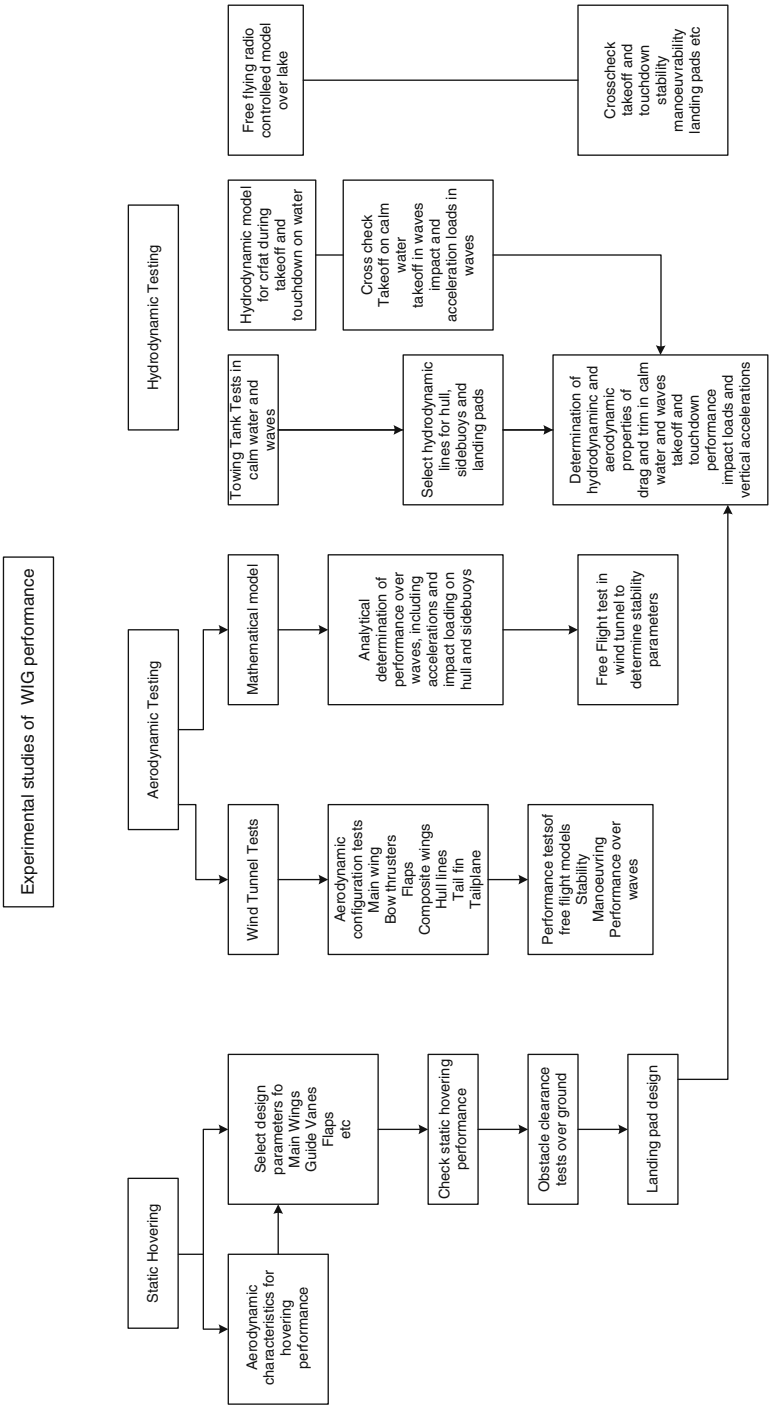


**Fig. 9.13** Block diagram for model testing and its relationship with preliminary design of WIG